China Petroleum Processing and Petrochemical Technology

Catalyst Research Volume 23, Issue 2, December 2023 Pp. 5157-5170

INVESTIGATION ON SURFACE INTEGRITY OF SS316L 3D PRINTED STENT

Mr. Rohit P. Jadhav

Ph.D. Scholar,Department of Mechanical Engineering, Sanjay Ghodawat University, Atigre, Kolhapur, 416118, Maharashtra, India,

Dr. Abhijit A. Patil

Assistant Professor, Department of Mechanical Engineering, Sanjay Ghodawat University, Atigre, Kolhapur, 416118, Maharashtra, India,

Abstract:

This investigation focuses on the analysis of the surface integrity of aStainless Steel 316L (SS316L) powder stent manufactured using Selective Laser Melting (SLM) technology. In the present work different post-processingmethods viz. stress-relieved, electropolished, stress-relieved and electropolished, and without stress-relieved and without electropolished were studied in correlation with the SLM process in the context of stent surface characterization. The process performances were evaluated in terms of surface roughness which is correlated with characterization techniques such as Scanning Electron Microscopy (SEM) and Electron Backscatter Diffraction (EBSD).It was observed that electropolished and stress-relieved stent exhibits lower average surface roughness Ra (0.484 μm), root mean square of the profile Rq (0.560 μm), total height of the roughness profile Rt (2.789 μm) and ten-point mean roughness of Rz (1.98 μm), as compared to remaining samples. The average grain size is observed to be 40 μm for the electropolished stress-relieved stent. The obtained results were corroborated by the surface topography, local misorientation angle, grain size, and grain orientation.The overall study exhibits that electropolished and stress-relieved stent surfacewas found to be suitable.

Keywords: CVD,Stent, Selective laser melting, SS316L, Surface roughness, Metallurgical aspects

1. Introduction: -

Numerous cardiovascular diseases (CVD) have become more prevalent recently, and an increasing number of people have early-stage heart disease. Each year, countless individuals need assistance in the fight against heart disease. The most often implemented cardiovascular therapies comprise coronary artery bypass graft (CABG), heart valve replacement or repair, pacemaker insertion, heart transplantation, maze surgery, and coronary angioplasty aimed at treating cardiovascular disease. Coronary artery bypass graft (CABG) and coronary angioplasty which are the most commonly used methods for treating illnesses related to blood flow to the heart [1,2].One of history's most important medical advancements was the discovery of coronary angioplasty. Through a procedure called coronary angioplasty, blood can once more flow to the heart by relaxing the constrictions in the coronary arteries. Andreas Grunting carried out the initial angioplasty in 1977 [3]. In this process, a catheter is inserted through a peripheral artery to deliver a balloon to the site of blood vessels narrowing. Following that, the balloon is forced to expand under pressure, which enlarges the vessel, increases lumen size, and enhances blood flow. One of the vital elements used in

coronary angioplasty is the stent. A stent is a small metal mesh tube that ensures the opened arteries will not narrow or close again [4-6].

Typically, stents are made of Stainless Steel 316 L (SS316 L), Tantalum (Ta), Nitinol (Ni-Ti), Platinum (Pr), Titanium (Ti), Cobalt-Chromium (Co-Cr), Magnesium Alloy (WE43), and Pure Iron. Stents are also made from biodegradable metals based on magnesium, iron, and zinc. SS316L is an austenitic chromium-nickel stainless containing a deliberate amount of molybdenum which generally increases and improves pitting resistance and possesses low radiopacity and a strong propensity for crevice corrosion, also its fatigue property provides adequate strength under cyclic load in a biological environment. As a result, SS316L is extensively used in biomedical implant applications, including cardiovascular stents, artificial heart valves, bone fixation, orthopedic implants, screws, pins, sutures, and steel threads used in the fixation of fractures [7-10].

As the demand for stents is increasing every year, currently various conventional and non-conventional manufacturing techniques are used in manufacturing the stent. Knitting, welding, braiding, and photochemical etching, micro-electro-discharge machining, electroforming are examples of stent manufacturing techniques. A higher percentage of stents are manufactured using laser cutting of the tubes [10-11]. Despite being used for the majority of stent manufacturing, still it is lacking in manufacturing customized and complex-shaped stents as stents made traditionally may fit most people or be one size fits all; nevertheless, certain medical conditions need specialized care. The powder bed fusion 3D printing technology stands out as an intriguing choice for this purpose, as it can be utilized to make stents straight from powder. The development of this technology has been the subject of significant research from academia and industry. 3D printing is an additive fabrication technique to produce 3D components. It has the potential to print tools and parts in the interim, zero waste, lower cost, and innate micro-manufacturing capacity, which compel it to be used for biomedical applications [12-14].

The surface integrity is vital for bioimplants manufactured by any conventional or non-conventional method. Surface integrity is defined as the inherent or enhanced surface conditions produced by a machining or other surface-generating operation. It is quantified by the mechanical, metallurgical, chemical, and topological state of the surface. Surface integrity and functional performance of manufactured components have been a significant proponent for developing new manufacturing processes [15]. Also, Grain structure plays a significant role in determining the mechanical properties of materials, particularly in metals and alloys. The grain structure significantly influences the mechanical properties of materials, including strength, ductility, toughness, hardness, fatigue resistance, and creep resistance. Finer grains generally promote higher strength, ductility, toughness, fatigue resistance, and creep resistance, while coarser grains may lead to lower values for these properties [16-18]. So it is important to analyze the surface produced by 3D printing concerning its application in bioimplants. Also, there is a lack of studies reported on surfaces originating in bioimplants due to the 3D printing process. Additionally, scarce research has been reported on the metallurgical elements of 3D-printed bioimplants.

This study examines the metallurgical properties and surface roughness characteristics of an SLM-fabricated SS316L stent. Specifically, the surface roughness was measured, and then scanning

Catalyst Research Volume 23, Issue 2, December 2023 Pp. 5157-5170

electron microscopy (SEM) and electron backscatter diffraction (EBSD) were used to evaluate the grain size, orientation, and local intergranular misorientation. The surface roughness characteristics of four different post-processed surfaces were evaluated, and the good surface quality of the stent was taken into further consideration for the metallurgical aspect to overcome the challenges connected with employing 3D printing to make bioimplants.

2. Materials and Method

This section includes stent design, material, manufacturing process, experimental set-up, post-processed methods, their parameters and levels, and surface measurements and characterization techniques.

2.1 Stent Design and Material

SS316L powder was used in experimentation because of its simplicity in production, biocompatibility, appropriate mechanical strength, and corrosion resistance qualities. A stent with the following dimensions: length 40 mm, exterior diameter 4 mm, inside diameter 3.5 mm, the axial gap between neighboring stents 3.69 mm, and strut thickness 0.5 mm, was the subject of experiments. The stent illustrated in Fig.1 was created using the CREO CAD tool and served as an input for the SLM process used in 3D printing. To ensure that the part receives support while being printed, the stent's design is closed-structured.

Figure 1.CAD model of stent prepared in CREO

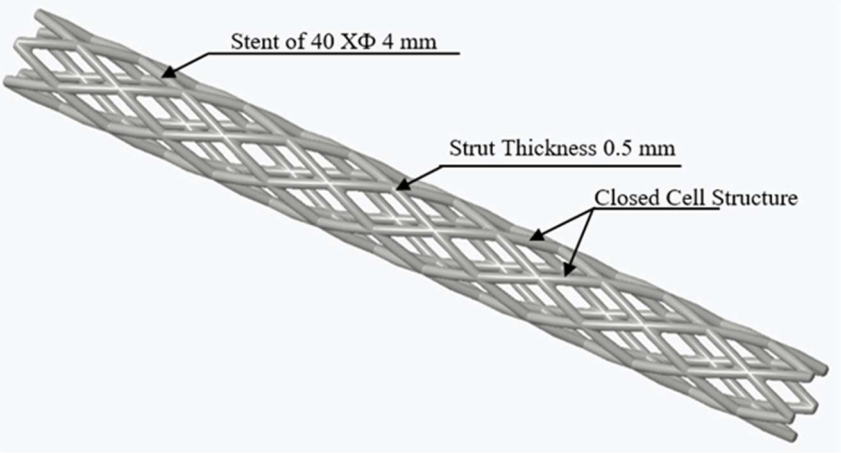

Table 1 lists the molecular composition of the SS316L powder used to create the stent. The powder used in this experimentation is prepared through a gas atomizing process (make: OEM). The powder used has a particle size range of 10 to 45 μm and a spherical particle shape. The powder had a bulk density of 7.95 g/cm3 and a thermal conductivity of 15 W/mK.

Table 1. Material composition of SS316L powder

Elements	Fe	N	C	S	P	Si	Mn	Mo	Ni	Cr
Wt.%	bal.	11.39	0.015	0.016	0.011	0.74	1.22	2.37	11.39	17.37

Catalyst Research Volume 23, Issue 2, December 2023 Pp. 5157-5170

2.2 SLM Setup

The industrial SLM system (make: SLM solutions SLM 280) was employed in the experimental 3D printing of the stent, as illustrated in Fig.2. Optimized input process parameters were taken into account in this work. Pre-pilot trials, preliminary experimentation, and a literature review are used to finalize the parameters. A constant layer thickness of 60 µm and height to aspect ratio of 1 mm were used in the printing of the stents. The device was configured to generate the stent at a maximum throughput of 113 cm3/h. The process used an average of 13 l/min of inert gas, with a beam focus of 80 µm and a scan speed of 10 m/s. Further sandblasting technique was used for cleaning the powder particles from the stent. These parameters were concerning supports as the part has a low thickness. Figure 3 shows SS316L stent manufactured on SLM 280 setup.

Figure 2. SLM 280 Setup

Figure 3. 3D Printed SS 316L powder stent with SLM process

2.3 Post-Processing Conditions

In this study, four samples of the stent, S1: stress-relieved, S2: electropolished, S3: stress- relieved and electropolished, and S4: without stress-relieved and without electropolished. For Sample S1heat treatment was carried out to relieve the stresses developed during the process, ramping up 150º per hour, holding at a temperature of 400º for two hours,and then cooling in the furnace. For Sample S2 electropolishing was carried out on the stent, the electrolyte temperature was 75º C. In the electrolyte, the perforated stainless steel cylinder served as a cathode. For electropolishing the value for current (I) = 0.6 to 0.75 A, temperature (T) = 75º C ± 2º C, and polishing time (t) = 30to 75 sec.The electrolyte commonly used for electropolishing SS316L stents is typically a mixture of sulfuric acid and phosphoric acid.Sample S4 was utilized in the investigation without any post-

Catalyst Research Volume 23, Issue 2, December 2023 Pp. 5157-5170

processing procedures, while sample S3 underwent both heat treatment and electropolishing procedures.

3. Results and Discussion

In this section, the obtained results of surface roughness, surface topography, and surface metallurgical aspects in terms of grain size, grain orientation, and local misorientation are discussed.

3.1 Surface Roughness

Surface roughness influences the interaction between stents and arteries, it is an essential feature of bioimplants[19]. In this study, four samples with an 80 µm sample profile length and a 10x to 80x lens set had their average surface roughness measured using a Bruker Alicona µCMM. Figure 4(a), illustrates stress-relieved stent, which have average surface roughness of Ra (0.546 µm), root mean square of the profile of Rq (0.692 µm), total height of the roughness profile of Rt (3.618 µm) and ten-point mean roughness of Rz (2.254 µm).From Fig. 4(b), electropolished stent had an average surface roughness of Ra (0.491 µm), root mean square of the profile of Rq (0.663 µm), total height of the roughness profile of Rt (3.115 µm) and ten-point mean roughness of Rz (2.32 µm).From Fig. 4(c), stress-relieved and electropolished stent had an average surface roughness of Ra (0.484 µm), root mean square of the profile of Rq (0.560 µm), the total height of the roughness profile of Rt (2.789 µm) and ten-point mean roughness of Rz (1.98 µm) and from Fig. 4(d), without stress-relieved and without electropolished stent had an average surface roughness of Ra (2.654 µm), root mean square of the profile of Rq (3.666 µm), total height of the roughness profile of Rt (16.915 µm) and ten-point mean roughness of Rz (7.842 µm). The stress-relieved and electropolished stent exhibited lower surface roughness as compared to other samples.

Figure 4. Surface parameters: (a) Stress-relieved, (b) Electropolished, (c) Stress-relieved and electropolished, and (d) Without stress-relieved and without electropolished

Figure 4(a). Stress-relieved

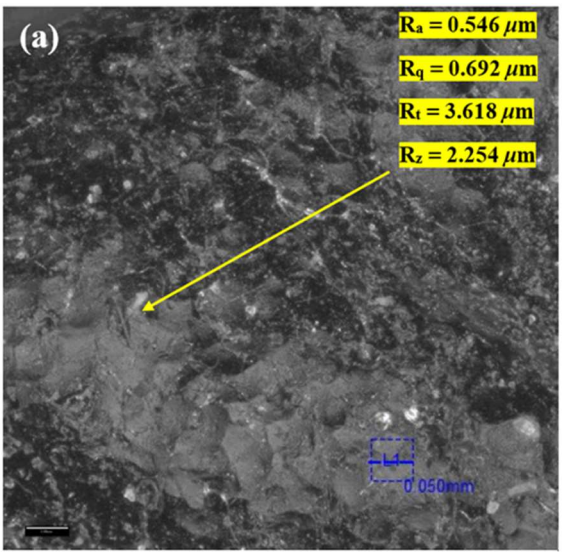

Catalyst Research Volume 23, Issue 2, December 2023 Pp. 5157-5170

Figure 4(b). Electropolished

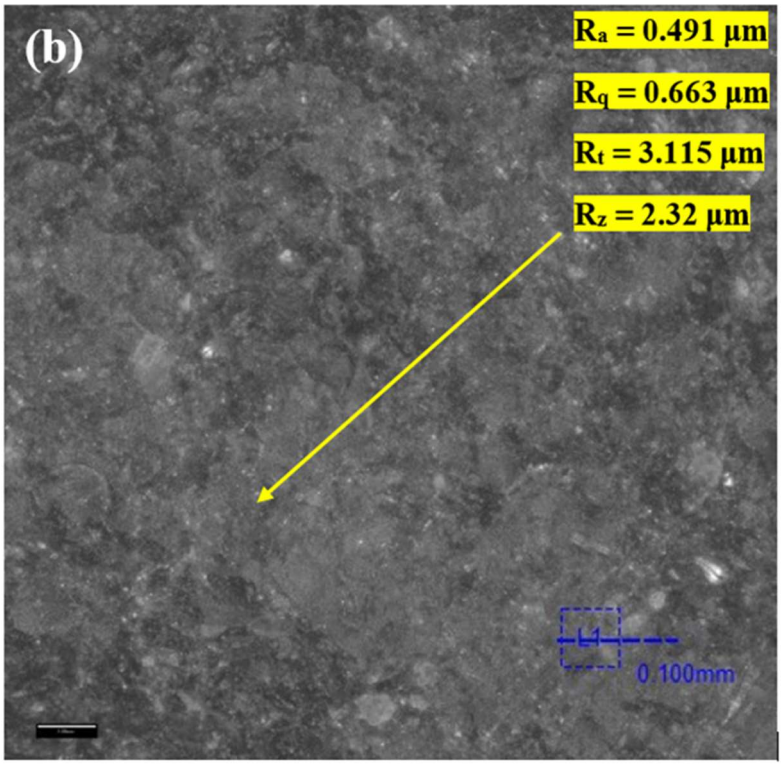

Figure 4(c). Stress-relieved and electropolished

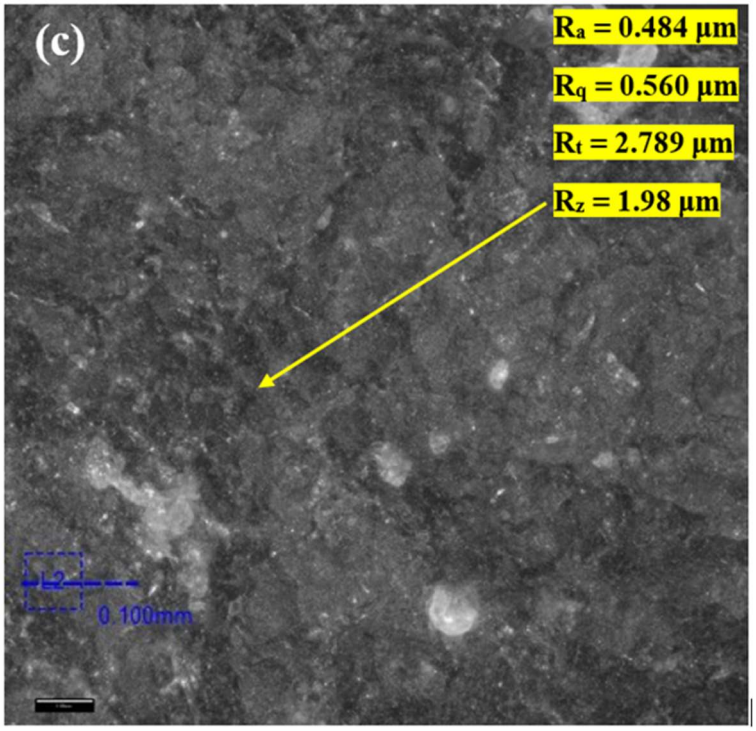

Figure 4(d). Without stress-relieved and without electropolished

Catalyst Research Volume 23, Issue 2, December 2023 Pp. 5157-5170

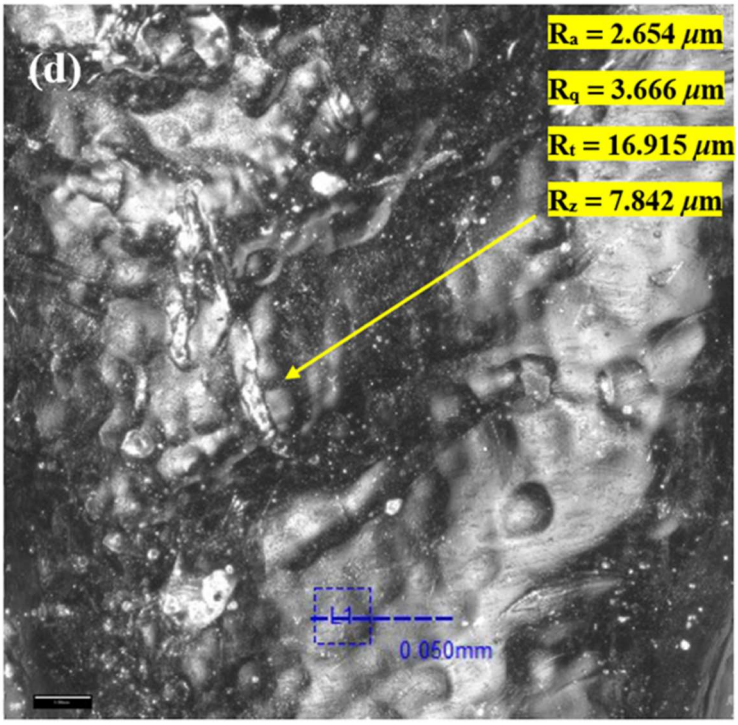

3.2 Surface Characterization

It is necessary to explore the surface morphology of the SS316L stent surfaces manufactured using the SLM technique, because several instances have been noted that were brought about by post-processing operations, viz., warpage, porosity, unmelted powder, micro-cracks, and particle deposition on the stent surface produced by the SLM process. SS316L powder stent surface morphology was investigated using SEM(make: ZEISS GeminiSEM 300). SEM was conducted along the length to examine the surface morphology at 1000x magnification. Figure 5(a) shows unmelted powder particles and microcracksover the stress-relieved stent surface. Most often a 3D printed parts undergoes stress-relieving, internal stresses that were present in the part are reduced or eliminated through controlled heating and cooling process. However, during this process, residual stresses are still present, particularly at the surface of the material.These stresses strive to exit the surface, resulting in the formation of microcracks [20]. The electropolished stent surface shows porous structure, shown in Fig. 5(b). Besides, Fig. 5(d) without stress-relieved and without electropolished stent exhibit deposition of powder particles on the surface. In contrast, smooth surface of the stress-relieved and electropolished stent is observed illustrated in Fig. 5(c). Because, the controlled heating and cooling eliminates process and material defects such as layer inconsistency, incomplete melting, inadequate powder bed formation, layer gaps, internal stresses, etc. These removal of defects gives even and good quality printing. Furthermore, optimized electropolishing removes unmelted particles, strays, metal deposition from the surface. Therefore, the combined effect of stress- relieving and electropolishing exhibits a better surface- quality.

Catalyst Research Volume 23, Issue 2, December 2023 Pp. 5157-5170

Figure 5. SEM images: (a) Stress-relieved, (b) Electropolished, (c) Stress-relieved and electropolished, and (d) Without stress-relieved and without electropolished.

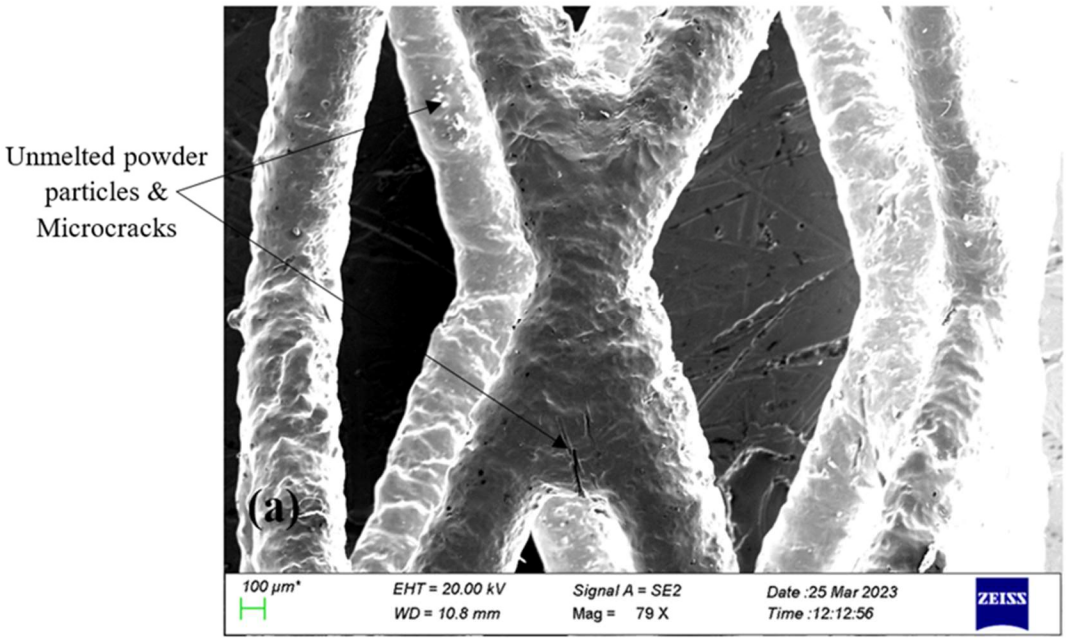

Figure 5(a). Stress-relieved

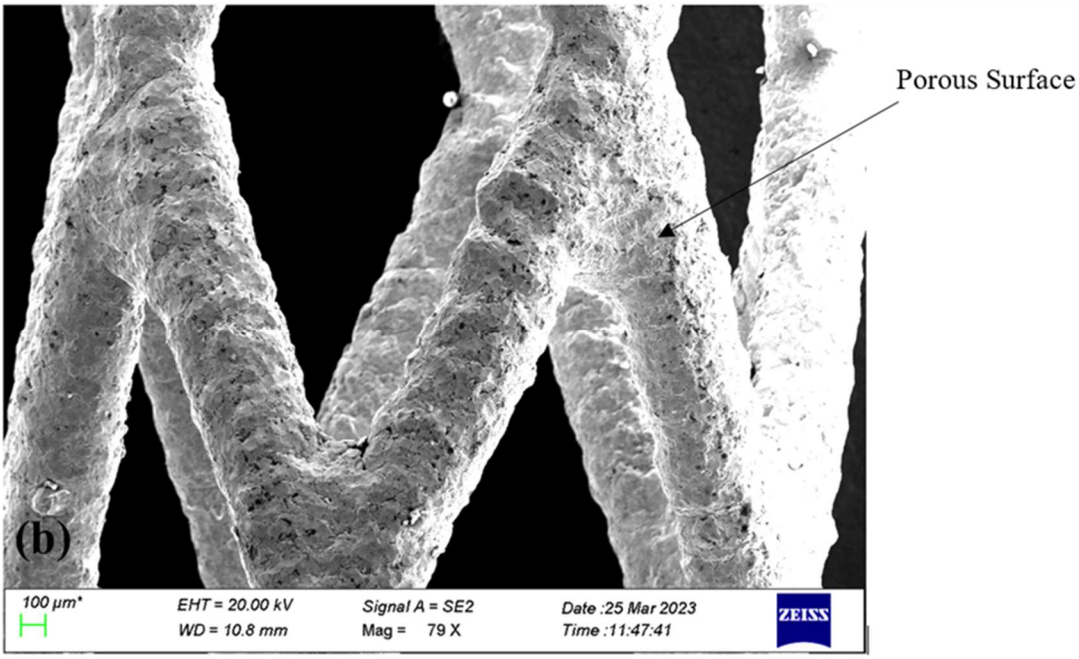

Figure 5(b). Electropolished

Catalyst Research Volume 23, Issue 2, December 2023 Pp. 5157-5170

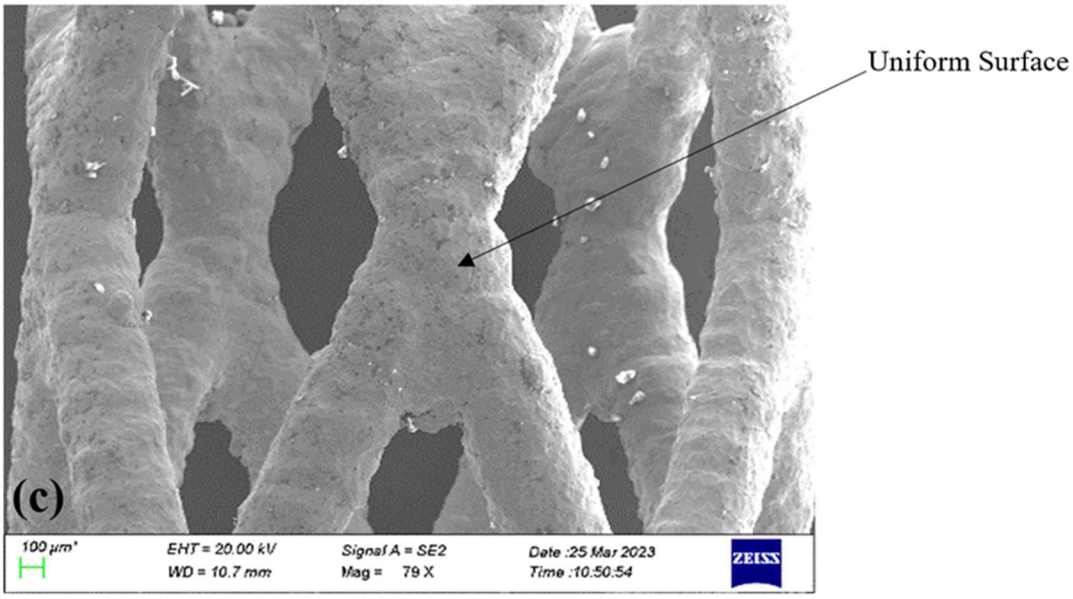

Figure 5(c). Stress-relieved and electropolished

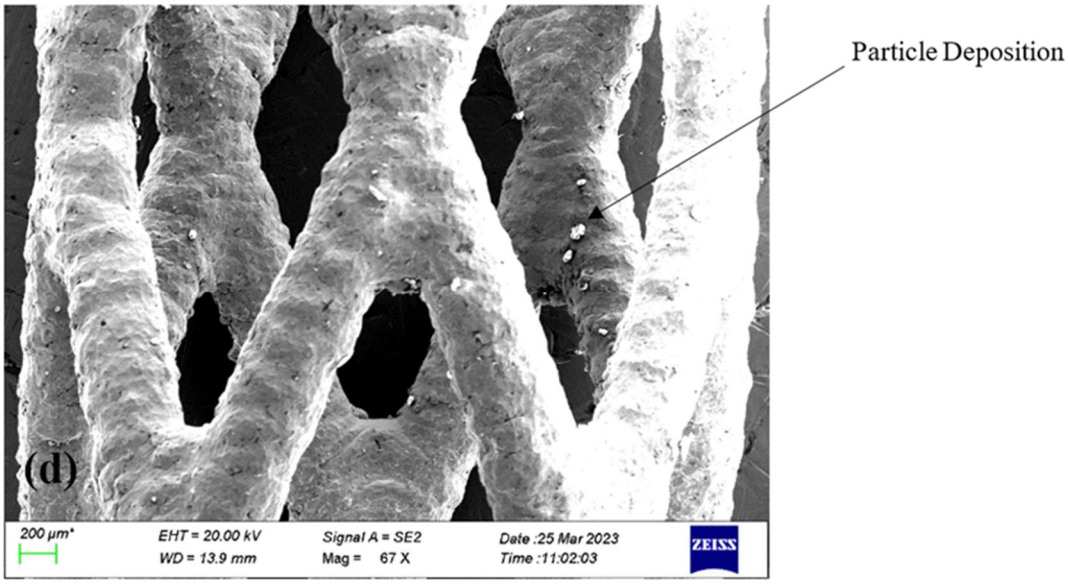

Figure 5(d). Without stress-relieved and without electropolished

3.3 Grain Size, Grain Orientation, and Misorientation Angle

The results observed from the surface roughness and surface characterization show that the stress-relieved and electropolished stent has improved surface quality as compared remaining samples. Therefore, it has been considered for further metallurgical analysis in the perspective of biomedical applications. Hence, the surface integrity of stress-relieved and electropolished stents is explored in terms of grain size, grain orientation, and misorientation angle [21]. For the preparation of the sample, the sample was grinded to remove surface imperfections and achieve a flat, polished surface. After grinding, the sample was polished using a series of finer abrasives to further refine

Catalyst Research Volume 23, Issue 2, December 2023 Pp. 5157-5170

the surface and remove any remaining scratches or defects. The final polish should produce a smooth, mirror-like surface suitable for EBSD analysis and finally, the sample was thoroughly cleaned to remove any debris, contaminants, or polishing residues that may interfere with the EBSD measurements.

Metallurgical properties, including composition, phase structure, and processing conditions, profoundly influence material behavior and performance. For instance, alloying elements can alter mechanical properties and corrosion resistance, while heat treatment can modify microstructure and grain size. In cell growth, metallurgical properties can affect surface chemistry, which in turn influences cell adhesion, proliferation, and differentiation. Certain metals or alloys may exhibit biocompatibility or bioactivity, promoting favorable interactions with cells [22].

Grain size refers to the size of individual crystals (grains) in a polycrystalline material. Smaller grain sizes typically result in higher strength and hardness due to grain boundary-strengthening mechanisms. In terms of cell growth, smaller grain sizes can inhibit the movement of dislocations, which are necessary for plastic deformation and thus can hinder cell formation. However, if there are preferred sites for nucleation at grain boundaries, smaller grains may enhance cell growth. The average grain size obtained of 3D printed stent is 40 μm as shown in Fig. 6(a). The suitability of a 40 μm grain for supporting cell growth depends on several factors, including the type of cells being cultured, the intended application, and the specific characteristics of the grains themselves. In general, cell growth and adherence can be influenced by the surface characteristics of the substrate, including its texture, chemistry, and porosity. While some cells may thrive on a substrate with a grain size of 40 μm, others may require a different surface texture or size for optimal growth.

Figure 6. (a) Grain size, (b) Grain Orientation, and (c) Misorientation angle of stress-relieved electropolished stent

Figure 6(a). Grain Size

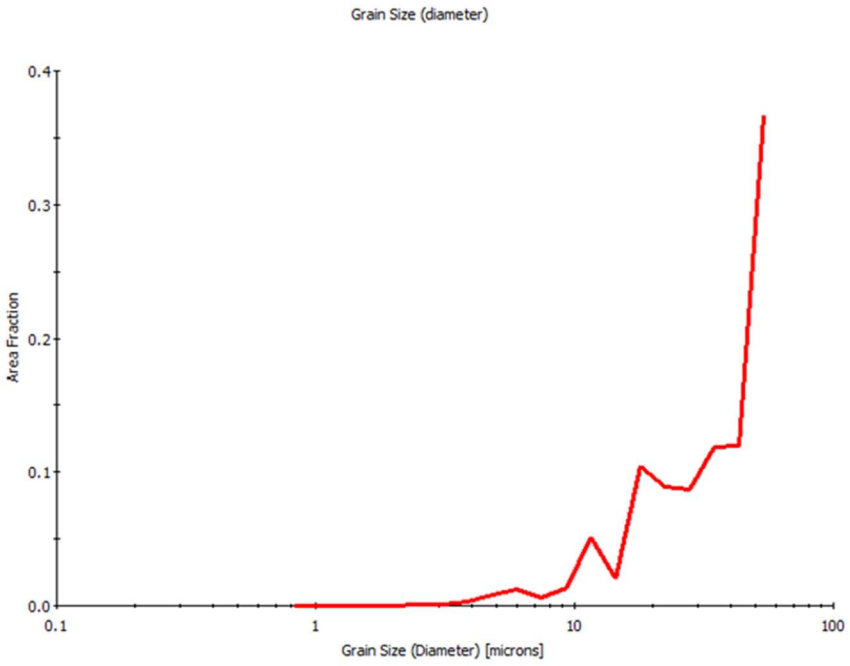

Catalyst Research Volume 23, Issue 2, December 2023 Pp. 5157-5170

The orientation of grains refers to the crystallographic orientation of adjacent grains. Certain crystal orientations can promote the formation of cells due to their effect on dislocation movement and grain boundary energy. Favorable orientations can lead to easier slip, facilitating the formation and propagation of cells. Practically all grains are oriented in the (001) plane which exhibits the lowest hardness and elastic modulus compared to plane (111) and (101). From Fig. 6(b) 19.91% and 15.53% of the grains have an orientation towards the (111) and (101) planes, respectively, and 64.56% of the grains have a heading towards the (001). Certain grain orientations, such as those that mimic the natural extracellular matrix (ECM) of tissues, can support cell adhesion, proliferation, and differentiation. For example, materials with anisotropic grain orientation, where the grains are aligned in a specific direction, can promote cell elongation and alignment along the same direction. This alignment can be beneficial for tissues like muscles or nerves, where directional cues are important for proper function. In general, materials with microstructures that resemble the native tissue ECM, including appropriate grain orientation, can provide cues for cells to attach, proliferate, and differentiate, thus supporting cell growth and tissue regeneration.

Figure 6(b). Grain orientation

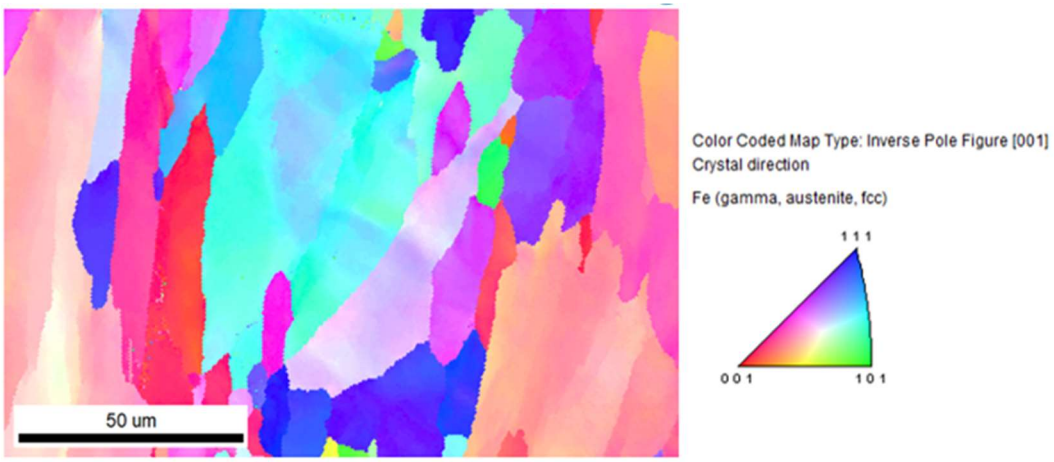

Figure 6(c). Misorientation angle

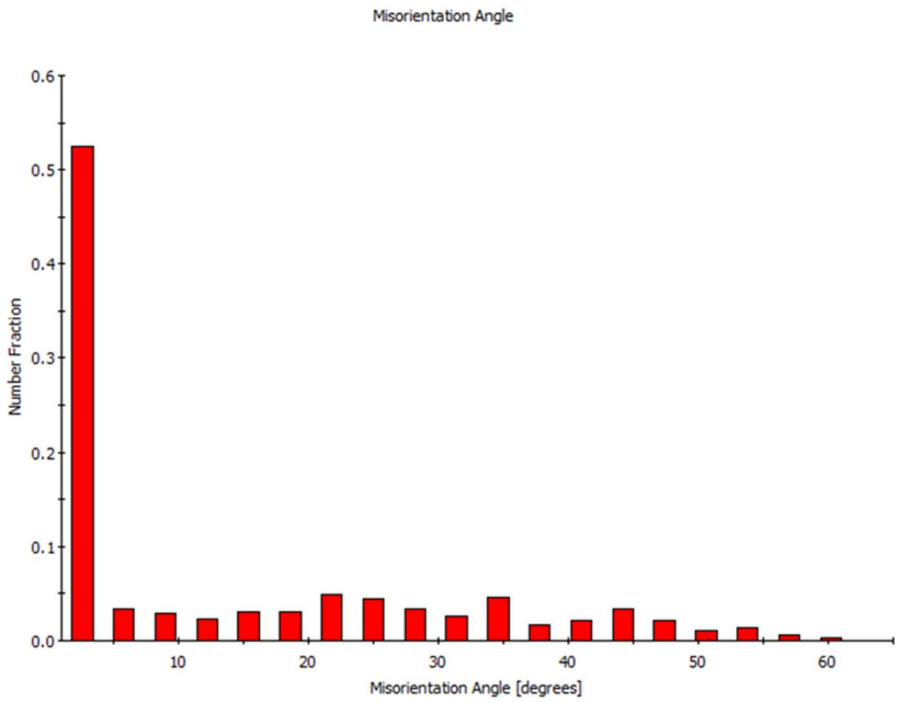

The misorientation angle refers to the angle between adjacent grains. Higher misorientation angles can lead to increased stored energy within the material, which can drive the formation of subgrains and subsequently cells. Dislocation pile-ups and interactions at high-angle grain boundaries can facilitate the formation of cells. The local grain misorientation of the electropolished and relieved stent stress is shown in Fig. 6(c). Local grain misorientation has a significant impact on the SLM process. Local grain misorientation was used to comparatively analyze the effects of the SLM procedure on surface roughness. The largest grain area fraction was discovered to be below the 5° grain misorientation angle, and roughly 64 % of the grain area fraction was found below the 15°. Overall, controlling factors in materials design (mechanical and metallurgical), facilitates the development with tailored properties specifically biomedical applications, such as stent

4. Conclusion: -

This study examined the impact of post-processing methods on surface roughness metrics and in extension, the optimized parameters are corroborated with metallurgical considerations such as grain size, grain orientation, and local misorientation in suitability with biomedical applications. From this examination following conclusions were drawn.

- The surface roughness parameters are more specific to exhibit surface quality. The surface parameters such as Ra 0.484 µm, Rq 0.560 µm, Rt 2.789 µm, and Rz 1.98 µm for stress-relievedand electropolished stent is found to be better. Whereas the surface roughness parameters as mentioned above are observed to be higher in the order of without stress relieved and without electropolished, electropolished and stress relieved, stent respectively.

- The evaluation of SEM images of surface topography of 3D printed stent surface corroborates the obtained surface parameters. The surface defects such as warpage, unmelted powder, metal deposition, and microcracks are observed in SEM images of without stress relieved and without electropolished, electropolished, and stress relieved, respectively.
- The SLM process has a significant impact on grain orientation and it exhibits the inverse relation with grain size. The average grain size is found to be 40 μm for the electropolished stress-relieved stent.
- Grain orientation which is important to study hardness and elastic modulus of the material, showed that grains were close to 001.

5. References

1. Yufeng Zheng, Hongtao Yang, Manufacturing of Cardio-vascular stents, Department of Materials Science Engineering, College of Engineering, Peking Beijing, P.R.China, Metallic Biomaterials Processing and Medical Device Manufacturing (2021), Pages 317-340.
2. Gupta R, Trends in Coronary Heart Disease Epidemiology in India, Jaipur, India; and New York, New York, Annals of Global Health, Vol 82 (2016), Pages 307-315.
3. Matthias Barton, Johannes Gruntzig, Balloon angioplasty – the legacy of Andreas Gruntzig, M.D (1939-1985), University of Zurich, Switzerland, Frontiers in Cardiovascular Medicine, Reviews in Medicine, Volume 1 (2014), Pages 1-25.
4. E. Langi, L.G. Zhao, P. Jamshidi, Microstructural and Mechanical Characterization of thin-walled tube manufactured by selective laser machining or stent application, Journal of Materials Engineering and Performance Volume 30(1) (2021), Pages 696-710.
5. Hendra Hirmawan, Process of prototyping coronary stents from biodegradable Fe–Mn alloys, ActaBiomaterialia, Volume 9, Issue 10, November 2013, Pages 8585-8592, https://doi.org/10.1016/j.actbio.2013.04.027
6. N. Muhammad, D. Whitehead, A. Boor, and L. Li, Comparison of Dry and Wet Fibre Laser Profile Cutting of Thin 316L Stainless Steel Tubes for Medical Device Applications, J. Mater. Process. Technol., (2010),210 (15), Pages 2261–2267.
7. V. Finazzi, A.G. Demir, C.A. Biffi, F. Migliavacca, L. Petrini, and B.Previtali, Design and Functional Testing of a Novel Balloon-Expandable Cardiovascular Stent in CoCr Alloy Produced by Selective Laser Melting, J. Manuf. Process., (2020), 55, Pages 161–173
8. AtulR. Saraf, Mudigonda Sadaiah, Photochemical machining of a novel cardiovascular stent, Materials and Manufacturing Processes, ISSN: 1042-6914 (Print) 1532-2475 (Online).
9. Kathuria Y.P, Biocompatible metallic stent for medical therapy, Department of Robotics, Faculty of Science and Engineering Ritsumeikan University Kusatsu-shi Shiga-ken 525-8577Japan, Vol 5287 (2003), Pages 52-61.
10. Shrikant Thorat, Rupesh Dugad, Sadaiah Mudigonda, Design Analysis and Manufacturing of Bare Metal Coronary Stent using PCM, Proceedings 10th International Conference on Precision, Meso, Micro, Nano Engineering (COPEN 10), (2017), IIT Madras, Pages 129-132.

Catalyst Research Volume 23, Issue 2, December 2023 Pp. 5157-5170

11. Deepakkumar Patil, Shrikant Thorat, Sadaiah Mudigonda, Study of the effect of PCM process parameters on geometry type, Ra, depth of etch, undercut comparing FeCl3 and CuCl2 etchants on Monel 400, Advances in Materials and Processing Technologies, (2023), Pages 1-21.
12. Wang, Ben. "The future of manufacturing: A new perspective." Engineering 4, no. 5 (2018): 722-728.
13. Juan Pou, Antonio Riveiro, J. Paulo Davim, Additive Manufacturing, Handbooks in Advanced Manufacturing, illustrated, Elsevier Science, 2021, 0128184116, 9780128184110.
14. Rupinder Singh, J. Paulo Davim, Additive Manufacturing Applications and Innovations, ISBN 9780367780944, 280 Pages, Published March 31, 2021 by CRC Press, Taylor and Francis.
15. Davim, J. Paulo, ed. Surface integrity in machining. Vol. 1848828742. London: Springer, 2010.
16. Shrikant Thorat, Sadaiah Mudigonda, The relative influence of surface metallurgy and self-magnetization induced by different manufacturing processes on surface integrity of Co-Cr alloy using PCM, Material Characterization, 167 (2020) 110526, https://doi.org/10.1016/j.matchar.2020.110526
17. Zhou, Wenbin, Jianguo Lin, Daniel S. Balint, and Trevor A. Dean. "Clarification of the effect of temperature and strain rate on workpiece deformation behavior in metal forming processes." International Journal of Machine Tools and Manufacture 171 (2021): 103815.
18. Zhou, Wenbin, Junquan Yu, Xiaochen Lu, Jianguo Lin, and Trevor A. Dean. "A comparative study on deformation mechanisms, microstructures and mechanical properties of wide thin-ribbed sections formed by sideways and forward extrusion." International Journal of Machine Tools and Manufacture 168 (2021): 103771.
19. E.S.Gadelmawla, Roughness Parameters, Production Engineering and Mechanical Design Department, Mansoura University, Egypt, Journal of Materials Processing Technology 123 (2002), Pages 133-145.
20. Raval Ankur, Choubey Animesh, Development and assessment of 316LVM cardiovascular stents, Research and Development Division, Sahajanand Medical Technologies, Surat 395003, India, (2004), Pages 331-343.
21. Shrikant Thorat, Sadaiah Mudigonda, The effect of residual stresses, grain size, grain orientation, and hardness on the surface quality of Co–Cr L605 alloy in Photochemical Machining. Journal of Alloys and Compounds 804 (2019), Pages 84-92.
22. Shrikant Thorat, Sadaiah Mudigonda, Investigation on surface integrity of Co-Cr L605 alloy in photochemical machining, Journal of Manufacturing Process 38 (2019), Pages 483-493.